Nanoscale

COMMUNICATION

Supplementary Information

Gas-generating nanoparticles for contrast-enhanced ultrasound imaging

In-Cheol Sun and Stanislav Emelianov *

Experimental Section

Preparation of glycol-chitosan-coated gold nanoparticles (GC-AuNPs) and 4-azidobenzoic acid (AzBA) conjugation

Gold(III) chloride trihydrate ($HAuCl_4 \bullet 3H_2O$), glycol chitosan (GC), 4-azidobenzoic acid (AzBA) solution (~0.2M), 1-ethyl-3-(3-dimethylaminopropyl) carbodiimide hydrochloride (EDC), and N-hydroxysuccinimide (NHS) were purchased from Sigma-Aldrich and used as received without any purification or modification. The synthesis of GC-AuNPs and the AzBA conjugation to GC were performed as described elsewhere.[1,2] Briefly, $HAuCl_4 \bullet 3H_2O$ solution (1 mM, 50 ml) was mixed with GC solution (1 mg/ml, 150 ml) at 70°C under stirring until the solution turned to red. Then, the solution was cooled down to room temperature and kept under stirring for 24 h. Then, 1 ml of GC-AuNP colloid was washed twice with centrifuge (10000 rpm, 20 min), dispersed in ethanol, and mixed with AzBA (0.2M, 0.01 ml), EDC (0.9585 mg), and NHS (0.5795 mg). The unreacted AzBA molecules were removed by centrifuge and the final concentration was adjusted to 5 X 10^{13} particles/ml (OD = 10). The stock solution was kept in dark.

Characterization of AzGC-AuNPs

FTIR spectrum, zeta potentials, UV-vis-NIR absorption, and morphology of AzGC-AuNPs were analysed with iS50 FT-IR Spectrometer (Thermo Scientific), Zetasizer Nano-ZS (Malvern), Evolution 220 (Thermo Scientific) spectrophotometer, and HT7700 (Hitachi) transmission electron microscope (TEM), respectively. Using the built-in ATR accessory, the FTIR spectrum of AzGC-AuNP colloid was directly measured after the removal of unreacted AzBA through centrifuge. Zeta potentials and size distribution were measured at 25°C from Zetasizer Nano-ZS, which used a 4 mW He–Ne laser operating with a wavelength of 633 nm and a detection angle of 173°. Each measurement consisted of 12 runs with default software parameter values. The main effects of surface modification were studied through ANOVA analysis. For size distribution, the intensity-averaged particle diameters were calculated with predefined parameters such as refractive index, viscosity, and dielectric constant available in the application software. UV-vis-NIR spectrum from 200 nm to 900 nm was measured in quartz cuvettes scanning. TEM samples were prepared by dropping 10 µl of AzGC-AuNP colloid onto carbon-coated, 200-mesh copper grids. Their images were taken from HT7700 operating at 100 kV. The generated gas bubbles were analysed with gas chromatograph. After a vial was filled with AzGC-AuNP colloid without residual air and sealed with a rubber septum, the vial was irradiated with laser upside down. The generated gas was collected with syringe and directly injected into the electron impact mass spectrometry system that consisted of Agilent 7890A GC instrument and Agilent 5975C VL MSD detector. The carrier gas was helium, and air samples of 10 µl were injected.

Quantification of 4-azidobenzoic acid (AzBA) on glycol-chitosan-coated gold nanoparticles (GC-AuNPs)

The reaction concentration of AzBA and GC-AuNPs were 0.002 M and 5 X 10^{13} particles/ml (OD = 10), respectively. After the EDC/NHS reaction, AzGC-AuNP colloid was centrifuged and the absorbance of unreacted AzBA (supernatant) was measured. From the standard curve (Figure S1b), the concentration of unreacted AzBA was 0.0015 M. Therefore, the number of AzBA molecules per GC-AuNP was calculated as:

$$\frac{0.0005\ M\ \times 6.02\ \times 10^{23}}{5\ \times 10^{13}\ particle/ml} = 6 \times 10^{3}\ molecules/particle$$

Gas generation by laser pulses, and ultrasound imaging

Prior to laser irradiation and ultrasound imaging experiments, the AzGC-AuNP stock solution was diluted with distilled water and the final concentration was adjusted to 1.25 X 10^{13} particle/ml (OD = 2.5). Then, AzGC-AuNP solution was poured into a glass tube (inner diameter: 5 mm) and gas generation after laser irradiation was recorded using digital camera. For contrast-enhanced ultrasound (CEUS) imaging, a polyethylene tube (Intramedic) with inner diameter of 0.28 mm was placed in the centre of a clear acrylic cuvette (10 cm × 10 cm × 10 cm) extending horizontally. Then, 200 µl of AzGC-AuNP colloid was injected into the tube using syringe. The horizontal laser beam (8 mm diameter) perpendicularly irradiated the tube with a 532 nm wavelength, which was produced by Nd:YAG Q-switched pulsed (8 ns pulse duration) laser (Vibrant 532-I, Opotek, Inc.). The laser energy was measured right after each experiment and

School of Electrical and Computer Engineering and Wallace H. Coulter Department of Biomedical Engineering, Georgia Institute of Technology and Emory University School of Medicine, 777 Atlantic Drive, Atlanta, GA 30332, USA
E-mail: stas@gatech.edu

controlled by different FL-Q delay time between 210 µs and 360 µs. After laser irradiation, the contrast enhancement was visualized using the Vevo® 2100 ultrasound imaging system with a 40 MHz ultrasound array transducer (VisualSonics, Toronto, Canada). The transducer was placed above the irradiated point of the tube such that the cross-section of the tube was imaged. For flow imaging, AzGC-AuNP colloid was injected in the tube (1.6 mm diameter) using syringe pump (Fusion 400, Chemyx) with the flow rate set to 200 µl/min or, given the tube diameter, 1.7 mm/s velocity. However, due to flexibility of tubes used in our setup, the flow velocity was measured independently using ultrasound images of flow. The frame by frame analysis of ultrasound images (Movie S4) determined that the true average flow velocity in our setup was 1.16 ± 0.17 mm/s. Once the laminar flow was fully developed in the tube, N_2 bubbles were generated with the laser and the movement of the bubbles was recorded with the ultrasound imaging system. The ultrasound images were analysed with open source video analysis software (Tracker, ver. 4.9.8), and the flow velocity profile was obtained.

Figures

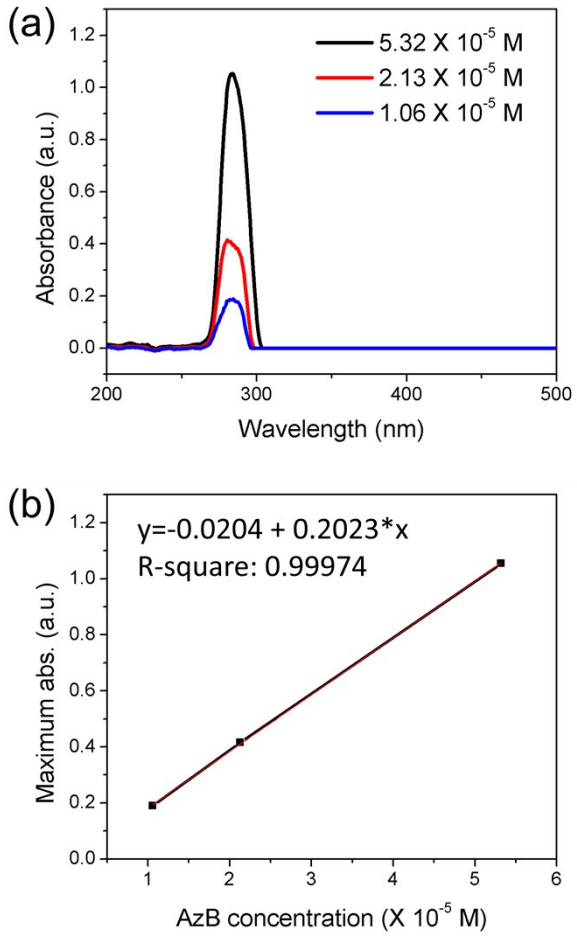

Figure S1. (a) UV-vis-NIR spectrum of AzBA solutions with different concentration. (b) Standard curve of maximum absorbance versus AzBA concentration.

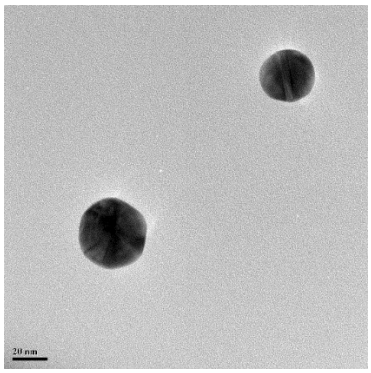

Figure S2. TEM image of AuNPs without surface coating.

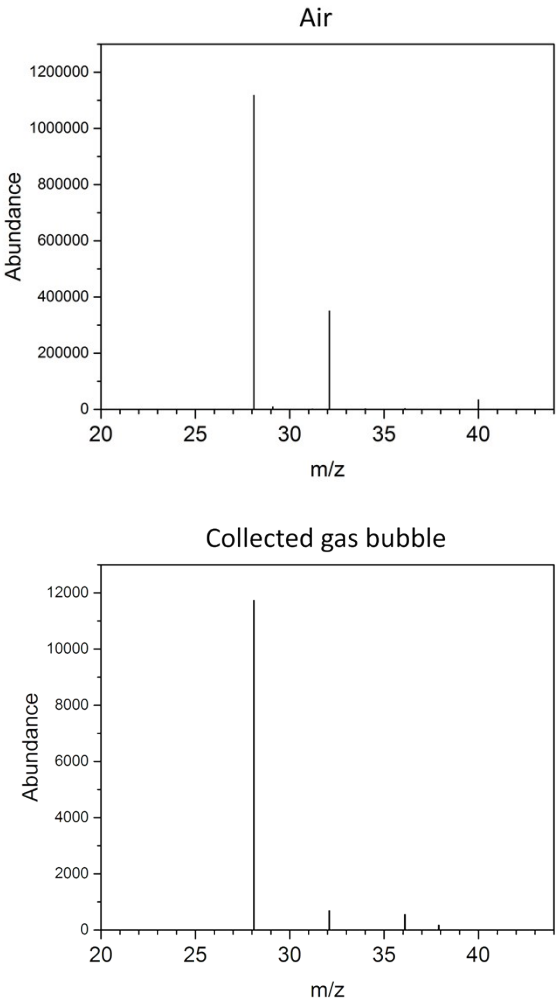

Figure S3. Mass spectra of air (control) and gas collected from sample of AzGC-AuNPs after laser irradiation. The small amount of oxygen in a sample with collected gas bubbles was from the dead volume of syringe and leakage of the chamber of GC-MS system.

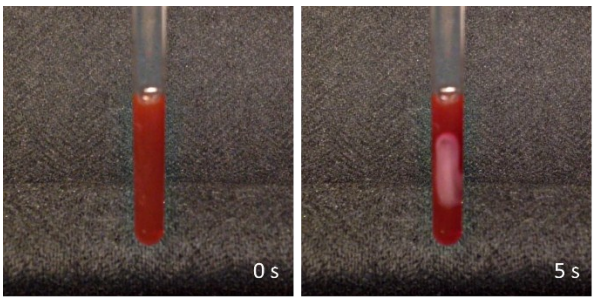

Movie S1. Real-time nitrogen gas generation from AzGC-AuNPs after laser irradiation. The stock solution of AzGC-AuNPs was diluted with distilled water and the final concentration was adjusted to 1.25 X 10^{13} particle/ml (OD = 2.5). Then, 0.3 ml of AzGC-AuNP colloid was poured into an NMR glass tube (inner diameter: 5 mm) and irradiated by single high energy laser pulse of Nd:YAG Q-switched laser (532 nm wavelength, 8 ns pulse duration, 8 mm beam diameter). The movie was recorded using digital camera. (AVI)

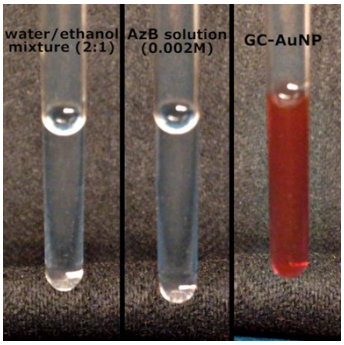

Movie S2. Laser irradiation on control groups. The experimental conditions are the same with Movie S1. [Left: water/ethanol solvent (2:1), middle: AzBA solution (0.002 M), right: GC-AuNP colloid without AzBA (1.25 X 10^{13} particle/ml, OD = 2.5)]. (AVI)

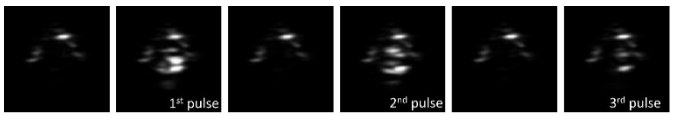

Movie S3. B-mode ultrasound imaging of on-demand gas generation by multiple laser pulses. The sample was irradiated with low energy laser pulses three times with the time interval of approximately one second. (AVI)

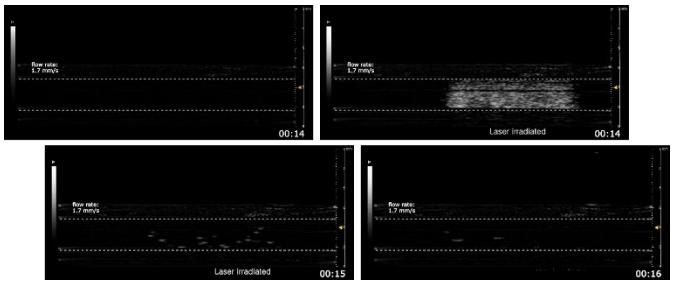

Movie S4. B-mode ultrasound imaging of N_2 generation under the laminar flow condition. Laminar flow (1.16 ± 0.17 mm/s) was created with a syringe pump (200 μl/min) in a tube (ID = 1.6 mm). (AVI)

References

1. I. C. Sun, D. K. Eun, H. Koo, C. Y. Ko, H. S. Kim, D. K. Yi, K. Choi, I. C. Kwon, K. Kim and C. H. Ahn, *Angew Chem Int Edit*, 2011, **50**, 9348-9351.
2. I. C. Sun, J. H. Na, S. Y. Jeong, D. E. Kim, I. C. Kwon, K. Choi, C. H. Ahn and K. Kim, *Pharmaceutical research*, 2014, **31**, 1418-1425.